ChemComm

Accepted Manuscript

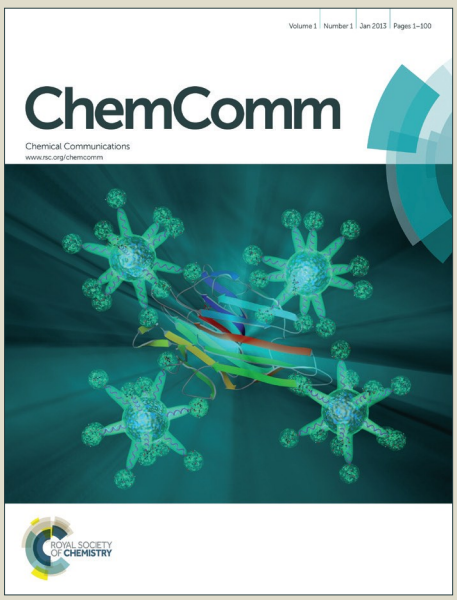

This is an *Accepted Manuscript*, which has been through the Royal Society of Chemistry peer review process and has been accepted for publication.

Accepted Manuscripts are published online shortly after acceptance, before technical editing, formatting and proof reading. Using this free service, authors can make their results available to the community, in citable form, before we publish the edited article. We will replace this *Accepted Manuscript* with the edited and formatted *Advance Article* as soon as it is available.

You can find more information about *Accepted Manuscripts* in the Information for Authors.

Please note that technical editing may introduce minor changes to the text and/or graphics, which may alter content. The journal's standard Terms & Conditions and the Ethical guidelines still apply. In no event shall the Royal Society of Chemistry be held responsible for any errors or omissions in this *Accepted Manuscript* or any consequences arising from the use of any information it contains.

ROYAL SOCIETY OF CHEMISTRY

www.rsc.org/chemcomm

Please do not adjust margins

ChemComm

COMMUNICATION

Performance enhancement of planar heterojunction perovskite solar cells by *n*-doping of electron transporting layer

Received 00th January 20xx,
Accepted 00th January 20xx

DOI: 10.1039/x0xx00000x

www.rsc.org/

Shin Sung Kim, Seunghwan Bae, and Won Ho Jo*

Herein we report a simple *n*-doping method to enhance the performance of perovskite solar cell with planar heterojunction structure. Device with *n*-doped PCBM electron transporting layer exhibits power conversion efficiency of 13.8% with a remarkably enhanced short-circuit current of 22.0 mA/cm^2 as compared to the device with un-doped PCBM layer.

Organic-inorganic hybrid perovskite has recently attracted enormous attention as the next generation material for solar cells because of its superior intrinsic properties such as extremely long exciton diffusion length, high absorption coefficient, and excellent charge carrier transport.[1] Dramatic enhancement of the power conversion efficiency (PCE) of perovskite solar cells has been achieved for the last few years.[2] Conventional n–i–p structure with mesoporous TiO_2/methylammonium lead trihalide perovskite ($CH_3NH_3PbX_3$, X = Cl^-, Br^-, I^-)/hole transporting material has widely been used and its PCE has currently exceeded 20%.[2e] However, since the formation of TiO_2 layer requires high temperature sintering process (>450 ℃), it is strongly needed to develop low-temperature and solution processable pervoskite solar cells. Very recently, planar heterojunction (PHJ) structure with a configuration of anode/hole transporting layer/perovskite/electron transporting layer (ETL)/cathode has attracted considerable attention because of its simple structure and low-temperature fabrication process.[3]

For PHJ perovskite solar cells, fullerene derivatives such as C_{60}, phenyl-C_{61}-butyric acid methyl ester (PCBM), $PC_{71}BM$, and indene-C_{60} bisadduct (ICBA) have commonly been used as ETL material because of their room temperature solubility and orthogonal solvent processability on the perovskite layer.[4] Thickness of ETL is very critical for achieving high performance of PHJ perovskite solar cells, because sufficiently thick ETL is required to prevent direct contact between rough perovskite layer and metal cathode.[3c] However, low electron mobility and low electrical conductivity of fullerene derivatives may limit the ETL thickness. When the thickness of PCBM was increased to 100 nm or thicker, the solar cell performance was notably diminished because of largely increased charge recombination.[5] Therefore, it is needed to increase the electrical conductivity of fullerene derivatives. One of effective ways to increase the electrical conductivity of fullerene is to dope or modify fullerenes, which may allow us to increase the ETL thickness and thus to achieve the performance enhancement of PHJ perovskite solar cells.

1,3-Dimethyl-2-phenyl-2,3-dihydro-1*H*-benzoimidazole (DMBI) has been reported as an effective *n*-type dopant for enhancing the electrical properties of *n*-type materials such as fullerene or naphthalene diimide (NDI) derivatives.[6] Since DMBI has good solubility in common organic solvents, the doping is easily achieved by simply mixing with *n*-type material in organic solvents. It has been reported that DMBI-doped PCBM films show remarkably increased electrical conductivity (from 8.1×10^{-8} S/cm to 1.9×10^{-3} S/cm) and enhanced air stability.[6a] It was also reported that the organic solar cell with DMBI-doped NDI-based ETL exhibited an enhanced PCE (from 0.69% to 3.42%).[6d] Despite of the effectiveness of DMBI derivatives as *n*-type dopant, the doping of DMBI to fullerene derivatives in organic solar cells has not been studied yet. Since the PHJ structure of perovskite solar cells contains PCBM layer as ETL, DMBI is expected to effectively dope the PCBM and thus to enhance the solar cell performance of perovskite solar cells.

In this report, we introduce an *n*-type dopant, DMBI, to dope the PCBM in perovskite solar cells with an inverted p–i–n structure. PCBM is effectively *n*-doped by simple mixing with DMBI, as clearly evidenced by up-shift of the Fermi level of PCBM upon addition of a small amount of DMBI. The solar cell device with *n*-doped PCBM ETL exhibits enhanced PCE with a remarkable enhancement of short-circuit current (J_{SC}) as compared to the device with un-doped PCBM layer. The increased electron transporting property of PCBM by *n*-doping decreases the series resistance and thus increases the fill factor (FF). The best device exhibits a high PCE of 13.8% with a J_{SC} of 22.0 mA cm^{-2} under illumination of AM 1.5 G 100 mW cm^{-2}. Especially, the effect of doping is more prominent when the thickness of PCBM layer is increased.

DMBI, an *n*-type dopant for ETL of PHJ perovskite solar cells, was synthesized by reacting *N*,*N*'-dimethyl-*o*-phenylenediamine with benzaldehyde according to the literature.[6c] Synthesized DMBI has

Department of Materials Science and Engineering, Seoul National University, 1 Gwanak-ro, Gwanak-gu, Seoul 151-744, Korea. E-mail: whjpoly@snu.ac.kr

† Electronic Supplementary Information (ESI) available: Detailed information about materials, characterizations and device fabrication. See DOI: 10.1039/x0xx00000x

ChemComm Accepted Manuscript

Please do not adjust margins

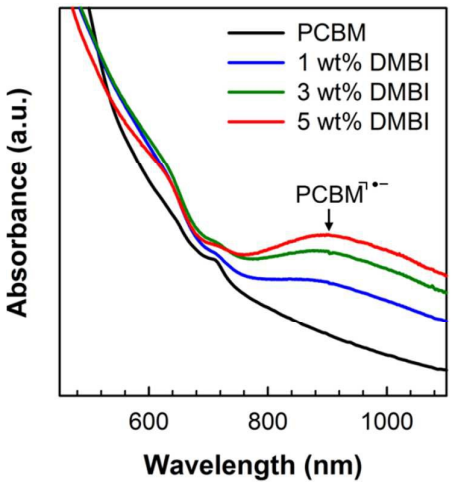

Fig. 1 UV-Vis-NIR absorption spectra of pure PCBM film and DMBI-doped PCBM films with various doping concentrations. All films are fabricated by spin-coating the chloroform solution on glass.

good solubility in common organic solvents such as chloroform and chlorobenzene, and therefore the *n*-doped PCBM layer is easily fabricated by spin-coating of a mixed solution of PCBM and DMBI in common solvent. The electrical conductivity of DMBI-doped PCBM film is 6.1×10^{-5} S/cm which is 4 orders of magnitude higher than that of pristine PCBM film (3.8×10^{-9} S/cm), as measured for the device with planar diode structure by a probe station (see Supplementary Information), indicating that the doping by DMBI increases largely the electrical conductivity of PCBM. When UV–Vis–NIR absorption spectra of pure PCBM and DMBI-doped PCBMs were measured and compared, as shown in Fig. 1, the DMBI-doped PCBM films exhibit a broad peak centered at 900 nm, while the peak intensity increases with the doping concentration, indicating that PCBM radical anions are formed in DMBI-doped PCBM.[7] Therefore, it is concluded that DMBI effectively dopes the PCBM in the simple mixture by donating an electron to PCBM.

The ultraviolet photoelectron spectroscopy (UPS) spectra were measured to examine the change of the Fermi level and the HOMO energy level with doping (Fig. 2). The work functions of films are determined by subtracting the binding energy cutoffs in high binding energy region (Fig. 2a) from the He I photon energy (21.22 eV), while the binding energy cutoffs in low binding energy region (Fig. 2b) indicate the energy gap between the Fermi levels and the HOMO energy level. The work function of PCBM is decreased from 5.04 eV to 4.78 eV upon addition of 1 wt% DMBI, as can be seen in Fig. 3c, and further addition of DMBI does not cause significantly further decrease of work function (Fig. 2a). In other words, an addition of DMBI shifts the Fermi level of PCBM toward the LUMO energy level, which is another evidence of *n*-doping. Therefore, the up-shift of the Fermi level due to *n*-doping of PCBM leads us to expect enhancement of electron transporting property of PCBM and thereby an increase in photocurrent of the solar cell device with *n*-doped PCBM ETL.

When the current density–voltage (*J*–*V*) curves of perovskite solar cells are measured with an inverted device configuration of

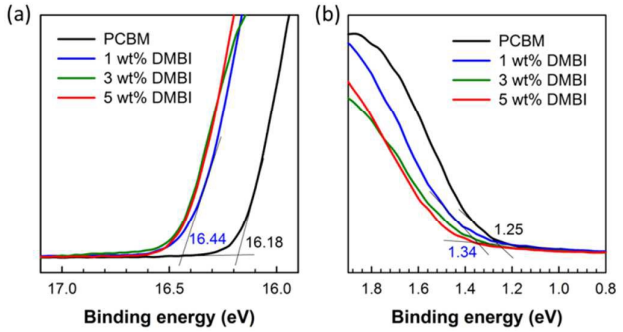

Fig. 2 UPS spectra of pure PCBM and DMBI-doped PCBM with various doping concentrations for (a) high binding energy region and (b) low binding energy region. Binding energy cutoffs of PCBM and PCBM doped with 1 wt% DMBI are indicated.

ITO/PEDOT:PSS/$CH_3NH_3PbI_3$/PCBM or PCBM:DMBI/Ca/Al (Fig. 3a), J_{SC} is notably enhanced by addition of DMBI to 50 nm-thick PCBM ETL, as shown in Fig. 4a and Table 1. The PCE is increased from 12.3% with a J_{SC} of 19.1 mA cm^{-2} to 13.0% with a J_{SC} of 21.0 mA cm^{-2}, when 1 wt% DMBI is added. Particularly, the increase of J_{SC} upon addition of 1 wt% DMBI is attributed to increased number of free electrons due to the up-shift of Fermi level. Increased electrical conductivity of DMBI-doped PCBM film is a clear evidence of this argument. When the addition of DMBI is further increased, both J_{SC} and V_{OC} remain nearly unchanged while FF is decreased, indicating that the optimum addition of DMBI is 1 wt%. The reason for the decrease of FF will be discussed later.

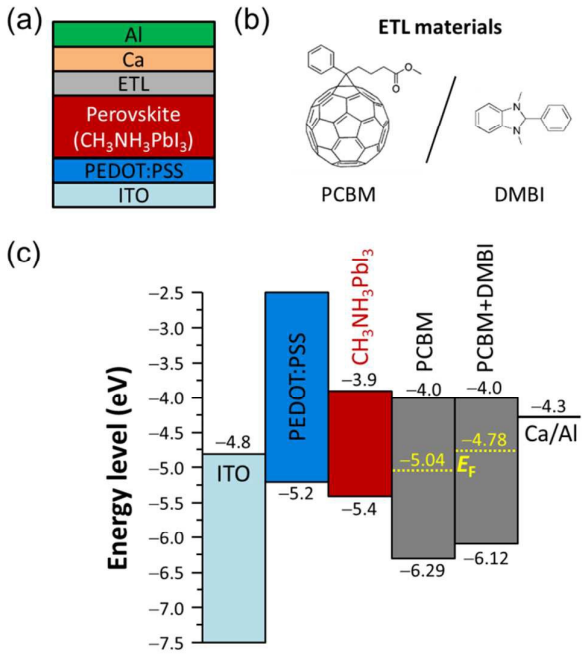

Fig. 3 (a) Schematic of the device architecture used in this work. (b) Chemical structure of PCBM and DMBI as ETL materials. (c) Energy levels of each layer. Fermi levels (E_F) and HOMO energy levels of ETL were determined for pure PCBM and 1 wt% doped PCBM by UPS measurements.

ChemComm Accepted Manuscript

This journal is © The Royal Society of Chemistry 20xx

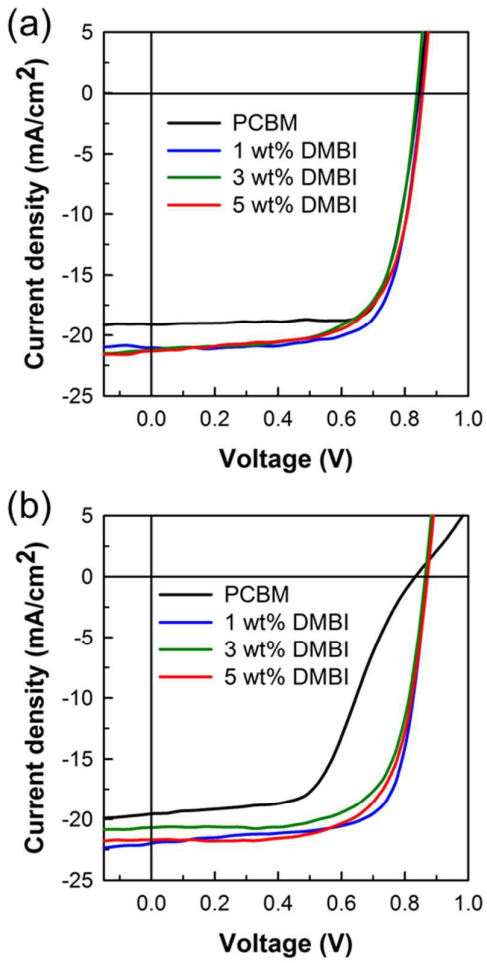

Fig. 4 *J*-*V* curves of the devices with (a) thin (50 nm) ETL which are fabricated by spin-coating of 10 mg/mL chloroform solution, and (b) thick (105 nm) ETL which are fabricated by spin-coating of 20 mg/mL chloroform solution.

Table 1 Photovoltaic properties of devices with PCBM ETL with different thickness and different dopant concentrations.

Sol. conc.[a] (mg/mL)	Dopant conc. of ETL	J_{SC} (mA cm^{-2})	V_{OC} (V)	FF	PCE[b] (%)
10	Pure PCBM	19.1	0.84	0.77	12.3 (11.0)
10	1 wt% DMBI	21.0	0.85	0.73	13.0 (12.1)
10	3 wt% DMBI	21.2	0.84	0.68	12.1 (11.1)
10	5 wt% DMBI	21.3	0.86	0.67	12.3 (11.1)
20	Pure PCBM	19.6	0.83	0.55	8.9 (7.9)
20	1 wt% DMBI	22.0	0.87	0.72	13.8 (12.2)
20	3 wt% DMBI	20.7	0.86	0.70	12.4 (11.2)
20	5 wt% DMBI	21.7	0.87	0.69	13.0 (11.6)

[a]10 and 20 mg/mL chloroform solutions are used for fabrication of 50 and 105 nm thick ETL, respectively.
[b]Average PCE values based on at least 10 devices are indicated in parentheses.

Fabrication of thick PCBM layer has an advantage of easy processing in industry while the increase of PCBM layer thickness decreases the PCE probably due to increased recombination and high series resistance, which arise mainly from low electrical conductivity of PCBM.[8] Hence, an increase of electrical conductivity of PCBM is essential for fabrication of thick PCBM layer without sacrifice of the device performance. Therefore, dramatically increased electrical conductivity of PCBM by *n*-doping may afford high PCE to the devices with thick PCBM layer. When one compares the doping effect on photovoltaic performance for thin PCBM (Fig. 4a) with that for thick PCBM layer (Fig. 4b), it reveals that the doping effect by DMBI is more remarkable for thick PCBM layer. As shown in Fig. 4b, the device with 105 nm-thick PCBM layer exhibits S-shaped *J*–*V* curve with a low FF of 0.55, while the device with 1 wt% DMBI-doped PCBM shows a remarkably improved FF of 0.72 probably due to reduced series resistance (Table S1), and as a result the PCE is increased from 8.9% (J_{SC}=19.6 mA cm^{-2} and V_{OC}=0.83 V) to 13.8% (J_{SC}=22.0 mA cm^{-2} and V_{OC}=0.87 V) upon addition of 1 wt% DMBI. The J_{SC} values calculated from external quantum efficiency spectra also show that J_{SC} increases when PCBM is doped by DMBI (see Fig. S1 and Table S1), which are very consistent with J_{SC}s measured from *J*–*V* curves within 5% error. Since it has been well recognized that the charge accumulation is the key factor for S-shaped curve,[9] the above result leads us to conclude that the doping by DMBI increases the electrical conductivity of PCBM and therefore prevents charge accumulation by generating free electrons in PCBM layer. In short, the addition of a small amount of DMBI (1 wt%) allows us to fabricate the devices with thick PCBM layer without loss of the solar cell performance.

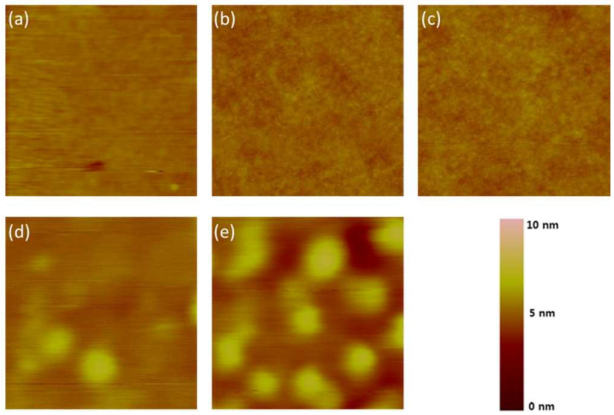

Fig. 5 AFM height images (1 μm × 1 μm scale) of (a) pure PCBM film, (b) 1 wt%, (c) 3 wt%, (d) 5 wt%, and (e) 10 wt% DMBI-doped PCBM film.

When the addition of DMBI is increased higher than 1 wt%, the FF of device is slightly decreased for both cases of thin and thick ETL, as shown in Table 1. The atomic force microscopy images of film surfaces have revealed that pristine PCBM film and 1 wt% doped PCBM film have smooth surface while PCBM films doped with 3 wt% and higher DMBI shows rough surface with large aggregates (Fig. 5). The rough surface inevitably causes poor contact between ETL and cathode, resulting in the increase of series resistance (Table S1). Hence, excessive doping may worsen the device performance, especially decrease the FF.

When we measure the hysteresis of devices, as shown in Fig. S2, we realize that all devices exhibit stable *J*–*V* curves without significant hysteresis with respect to the scan direction. However, the devices with high doping concentration (>3 wt%) exhibit weak hysteresis. Although the origin of hysteresis has not clearly been

ChemComm Accepted Manuscript

identified, the trap sites, ferroelectric properties of pervoskite and ion migration have been proposed as possible reasons. Hence, we have assumed that the hysteresis of our devices with high doping concentration is caused by an increase of trap sites due to DMBI doping.

In summary, we first introduced an *n*-type dopant, DMBI, to dope the PCBM ETL in PHJ perovskite solar cells. PCBM was effectively doped by DMBI, which was evidenced by UV–Vis–NIR absorption and UPS measurements. Solar cell devices with *n*-doped PCBM ETL exhibit higher PCE with remarkably increased J_{SC} as compared to un-doped device mainly due to the up-shift of Fermi level of PCBM. The best device shows a high PCE of 13.8% with a J_{SC} of 22.0 mA cm^{-2}. Furthermore, since the effect of DMBI-doping on photovoltaic performance is more prominent for the device with thicker PCBM layer, this method allows us to fabricate thicker ETL layer, which has a benefit of industrial processing of device fabrication. In short, this simple doping method can be an effective strategy for enhancing the performance of PHJ perovskite solar cells.

The authors thank the Ministry of Education, Korea for financial support through Global Research Laboratory (GRL). The authors also thank Mr. Tae Gun Kim for UPS measurement.

Notes and references

1 (a) J. -H. Im, C. -R. Lee, J. -W. Lee, S. -W. Park and N.-G. Park, *Nanoscale*, 2011, **3**, 4088-4093; (b) S. D. Stranks, G. E. Eperon, G. Grancini, C. Menelaou, M. J. P. Alcocer, T. Leijtens, L. M. Herz, A. Petrozza and H. J. Snaith, *Science*, 2013, **342**, 341–344; (c) G. Xing, N. Mathews, S. Sun, S. S. Lim, Y. M. Lam, M. Grätzel, S. Mhaisalkar and T. C. Sum, *Science*, 2013, **342**, 344–347; (d) E. Edri, S. Kirmayer, A. Henning, S. Mukhopadhyay, K. Gartsman, Y. Rosenwaks, G. Hodes and D. Cahen, *Nano Lett*., 2014, **14**, 1000–1004; (e) M. A. Green, A. Ho-Baillie and H. J. Snaith, *Nat*. *Photonics*, 2014, **8**, 506-514; (f) T. Leijtens, S. D. Stranks, G. E. Eperon, R. Lindblad, E. M. J. Johansson, I. J. McPherson, H. Rensmo, J. M. Ball, M. M. Lee and H. J. Snaith, *ACS Nano*, 2014, **8**, 7147–7155; (g) H. Oga, A. Saeki, Y. Ogomi, S. Hayase and S. Seki, *J. Am*. *Chem*. *Soc*., 2014, **136**, 13818-13825; (h) G. E. Eperon, S. D. Stranks, C. Menelaou, M. B. Johnston, L. M. Herz and H. J. Snaith, *Energy Environ*. *Sci*., 2014, **7**, 982-988.

2 (a) N. -G. Park, *J. Phys*. *Chem*. *Lett*., 2013, **4**, 2423-2429; (b) J. Burschka, N. Pellet, S. -J. Moon, R. Humphry-Baker, P. Gao, M. K. Nazeeruddin and M. Grätzel, *Nature*, 2013, **499**, 316-319; (c) H. Zhou, Q. Chen, G. Li, S. Luo, T. -B. Song, H. -S. Duan, Z. Hong, J. You, Y. Liu and Y. Yang, *Science*, 2014, **345**, 542-546; (d) N. J. Jeon, J. H. Noh, W. S. Yang, Y. C. Kim, S. Ryu, J. Seo and S. I. Seok, *Nature*, 2015, **517**, 476-480; (e) W. S. Yang, J. H. Noh, N. J. Jeon, Y. C. Kim, S. Ryu, J. Seo and S. I. Seok, *Science*, 2015, **348**, 1234-1237.

3 (a) P. Docampo, J. M. Ball, M. Darwich, G. E. Eperon and H. J. Snaith, *Nat*. *Commun*., 2013, 4:2761. DOI: 10.1038/ncomms3761; (b) S. Sun, T. Salim, N. Mathews, M. Duchamp, C. Boothroyd, G. Xing, T. C. Sum and Y. M. Lam, *Energy Environ*. *Sci*., 2014, **7**, 399-407; (c) J. You, Z. Hong, Y. Yang, Q. Chen, M. Cai, T. -B. Song, C. -C. Chen, S. Lu, Y. Liu, H. Zhou and Y. Yang, *ACS Nano*, 2014, **8**, 1674-1680; (d) J. -Y. Jeng, K. -C. Chen, T. -Y. Chiang, P. -Y. Lin, T. -D. Tsai, Y. -C. Chang, T. -F. Guo, P. Chen, T. -C. Wen and Y. -J. Hsu, *Adv*. *Mater*., 2014, **26**, 4107-4113; (e) F. Guo, H. Azimi, Y. Hou, T. Przybilla, M. Hu, C. Bronnbauer, S. langner, E. Spiecker, K. Forberich and C. J. Brabec, *Nanoscale*, 2015, **7**, 1642-1649; (f) W. Nie, H. Tsai, R. Asadpour, J. -C. Blancon, A. J. Neukirch, G. Gupta, J. J. Crochet, M. Chhowalla, S. Tretiak, M. A. Alam, H. -L. Wang and A. D. Mohite, *Science*, 2015, **347**, 522-525; (g) W. Chen, Y. Wu, J. Liu, C. Qin, X. Yang, A. Islam, Y. -B. Cheng and L. Han, *Energy Environ*. *Sci*., 2015, **8**, 629-640; (h) J. Min, Z. -G. Zhang, Y. Hou, C. O. R. Quiroz, T. Przybilla, C. Bronnbauer, F. Guo, K. Forberich, H. Azimi, T. Ameri, E. Spiecker, Y. Li and C. J. Brabec, *Chem*. *Mater*., 2015, **27**, 227-234; (i) X. Liu, H. Yu, L. Yan, Q. Dong, Q. Wan, Y. Zhou, B. Song and Y. Li, *ACS Appl*. *Mater*. *Interfaces*, 2015, **7**, 6230-6237.

4 (a) J. -Y. Jeng, Y. -F. Chiang, M. -H. Lee, S. -R. Peng, T. -F. Guo, P. Chen and T. -C. Wen, *Adv*. *Mater*., 2013, **25**, 3727-3732; (b) C. -H. Chiang, Z. -L. Tseng and C. -G. Wu, *J. Mater*. *Chem*. *A*, 2014, **2**, 15897-15903; (c) P. -W. Liang, C. -C. Chueh, S. T. Williams and A. K. -Y. Jen, *Adv*. *Energy Mater*., 2015, **5**, 1402321; (d) T. Salim, S. Sun, Y. Abe, A. Krishna, A. C. Grimisdale and Y. M. Lam, *J. Mater*. *Chem*. *A*, 2015, **3**, 8943-8969.

5 S. Ryu, J. Seo, S. S. Shin, Y. C. Kim, N. J. Jeon, J. H. Noh and S. I. Seok, *J. Mater*. *Chem*. *A*., 2015, **3**, 3271-3275.

6 (a) P. Wei, J. H. Oh, G. Dong and Z. Bao, *J. Am*. *Chem*. *Soc*., 2010, **132**, 8852-8853; (b) P. Wei, T. Menke, B. D. Naab, K. Leo, M. Riede and Z. Bao, *J. Am*. *Chem*. *Soc*., 2012, **134**, 3999-4002; (c) B. D. Naab, S. Guo, S. Olthof, E. G. B. Evans, P. Wei, G. L. Millhauser, A. Kahn, S. Barlow, S. R. Marder and Z. Bao, *J. Am*. *Chem*. *Soc*., 2013, **135**, 15018-15025; (d) N. Cho, H. -L. Yip, J. A. Davies, P. D. Kazarinoff, D. F. Zeigler, M. M. Durban, Y. Segawa, K. M. O'Malley, C. K. Luscombe and A. K.-Y. Jen, *Adv*. *Energy Mater*., 2011, **1**, 1148-1153.

7 (a) D. M. Guldi, H. Hungerbuhler, E. Janata and K.-D. Asmus, *J. Phys*. *Chem*., 1993, **97**, 11258-11264; (b) D. M. Guldi and M. Prato, *Acc*. *Chem*. *Res*., 2000, **33**, 695-703.

8 J. Seo, S. Park, Y. C. Kim, N. J. Jeon, J. H. Noh, S. C. Yoon and S. I. Seok, *Energy Environ*. *Sci*., 2014, **7**, 2642-2646.

9 J. C. Wang, X. C. Ren, S. Q. Shi, C. W. Leung and P. K. L. Chan, *Org*. *Electron*., 2011, **12**, 880-885.

ChemComm Accepted Manuscript

 This journal is © The Royal Society of Chemistry 20xx